Electronic Supplementary Information

A practical method for fabricating superparamagnetic films and the mechanism involved

Pei-Cheng Jiang,[1,2,#] Cheng-Hsun-Tony Chang,[3,#] Chen-Yuan Hsieh,[1] Wei-Bin Su,[2] and Jyh-Shen Tsay[1,*]

[1]*Department of Physics, National Taiwan Normal University, Taipei 116, Taiwan*

[2]*Institute of Physics, Academia Sinica, Taipei 11529, Taiwan*

[3]*Department of Electronic Engineering, Minghsin University of Science and Technology, Hsinchu 30401, Taiwan*

Blocking temperature

Magnetic properties of Co/Ir(111) were investigated by employing SQUID magnetometry. As an example for 8 ML Co/Ir(111), ZFC and FC curves collected at H = 50 Oe are shown in Figure S1. The curves display the typical behavior of superparamagnetic materials. The blocking temperature T_B, corresponding to the maximum in the ZFC curve, falls in the temperature range between 120 and 160 K. At temperature below T_B, the spins freeze and the system enter the blocked regime with typical out-of-equilibrium behavior [1-5]. The measured blocking temperature of 8 ML Co/Ir(111) is much higher than what we expected. This phenomenon has been previously observed for superparamagnetic nanoparticles in this size range (~1 nm^3) and are attributed to a significantly higher value of magnetocrystalline anisotropy [5-7].

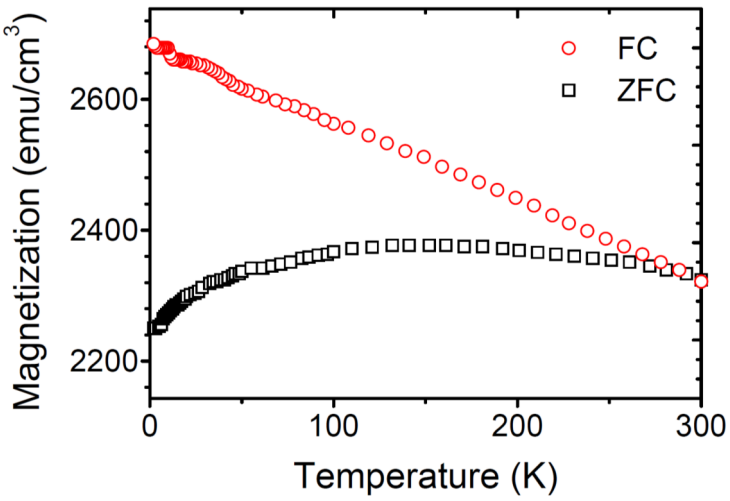

Figure S1. Field cooled (FC) and zero-field cooled (ZFC) curves for 8 ML Co/Ir(111).

SPM cluster size

From the literature, the median magnetic diameter of superparamagnetic nanoparticles can be calculated from the magnetic measurements [8-11]. As reported by Ferrari et al, the median magnetic moment of the particle can be calculated by refining the high temperature anhysteretic magnetization isotherms, using the Langevin function with a unimodal log-normal distribution [9,10]. For the real system of the superparamagnetic nanoparticles with a size distribution, the magnetization M of the nanoparticles in a magnetic field H can be written as a weighted sum of the Langevin functions [9,10]

$$M(H,T) = \int_0^\infty \mu L\left(\frac{\mu H}{k_B T}\right) f(\mu)\, d\mu + X_{linear} H \qquad \text{(S1)}$$

where $f(\mu)$ is the distribution function of magnetic moments μ in a system of superparamagnetic grains, k_B is the Boltzmann constant. In Equation S1, the second term is related to additional linear contribution to the magnetization and can be originated from diamagnetic or paramagnetic components of the sample with magnetic susceptibility X_{linear}. By taking the unimodal log-normal distribution of the magnetic moments μ, the distribution function $f(\mu)$ can be expressed as follows

$$f(\mu) = \frac{1}{\sqrt{2\pi}\mu\sigma} exp\left(-\frac{ln^2\left(\frac{\mu}{\mu_0}\right)}{2\sigma^2}\right), \quad \mu_m = \mu_0 exp\frac{\sigma^2}{2} \qquad \text{(S2)}$$

where σ is the distribution width, μ_0 and μ_m are the median and mean magnetic moment, respectively. The distribution function $f(\mu)$ can be obtained from the refinement of the magnetization isotherm measured above T_B in the Octave software using Equation S1 [9,10].

The fitting curve of the magnetization $M(H,T)$ is shown in Figure S2. We may consider $\mu_x = M_V V_x$ (x=0 or m) where the M_V is the magnetization per volume [11]. The volume distribution function $f(V_\mu)$ of superparamagnetic clusters as shown in the inset in Figure S2 was calculated from the $f(\mu)$ by taking $V_x = \mu_x / M_V$ into account. From the volume distribution function $f(V_\mu)$ calculated from the M-H curve for 8 ML Co/Ir at 300 K, the median volume V_o and mean volume V_m of the superparamagnetic clusters are determined to be 1.236 and 1.242 nm^3, respectively. As compared to the STM measurements (V_{STM}= 1.17±0.14 nm^3) as discussed in Figure 2, a well consistence of the determined volume is obtained.

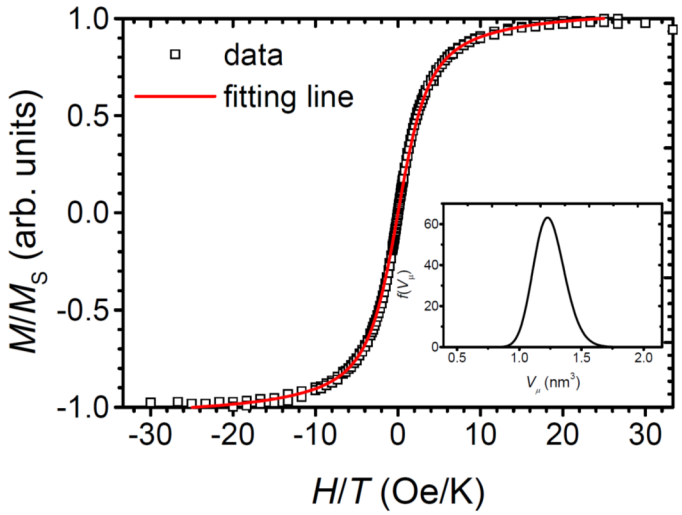

Figure S2. Magnetization isotherms for 8 ML Co/Ir(111) as measured at 300 K and plotted in generalized Langevin scaling. The inset shows the volume distribution $f(V_\mu)$ of superparamagnetic clusters.

Superparamagnetic film on a microchip (SFoM)

Based on the method reported herein for producing superparamagnetic films, we propose a superparamagnetic film on a microchip (SFoM) in which the total magnetic moment can be further enhanced by 500 times as compared to commercial MRI contrast agents, which use superparamagnetic nanoparticles. The schematic plot in Figure S3 shows a comparison of the total magnetic moments for MRI measurements by estimating the total population of magnetic atoms [12,13] of commercial MRI contrast agents and the SFoM. Because the amount of antigenic epitopes on the surface of typical circulating tumor cell (CTC), the number of bonding MRI contrast agents is limited to between several to a few hundred, depending on the size and species of the antigen [14-16]. The sizes of the superparamagnetic nanoparticles in commercial MRI contrast agents are typically between 20 and 400 nm^3 [17-19] which correspond to 1800 and 36000 atoms, respectively. If we take the number of bonding MRI contrast agents on the surface of a CTC to be one hundred, the total magnetic moment for MRI measurements corresponds to contributions from 180 thousand to 3.6 million atoms on a CTC surface in the case of commercial MRI contrast agents. Concerning SFoM based on the extreme chip technology in use today, the minimum diameter of microchip can be as small as 10 μm [20] and its volume is approximately equivalent to that for a leukocyte [21]. For a nanocluster produced by strain accumulation and relaxation in the specimens, the typical size is around one nm^3, a volume that could contain 90 atoms. Although the sizes of the nanoclusters are smaller, the areal density is condensed on the substrate to a considerable extent. Based

on our STM measurements, there are 125 nanoclusters in a 25×25 nm^2 image. For SFoM, the total magnetic moment for MRI measurements corresponds to contributions from 1.8 billion atoms on a single microchip. This makes the total magnetic moment for SFoM to be 500 times larger than that of commercial MRI contrast agents using superparamagnetic nanoparticles. Because of the larger total magnetic moment, the SFoM would pave the way for further strategies for fabricating biosensors on a microchip.

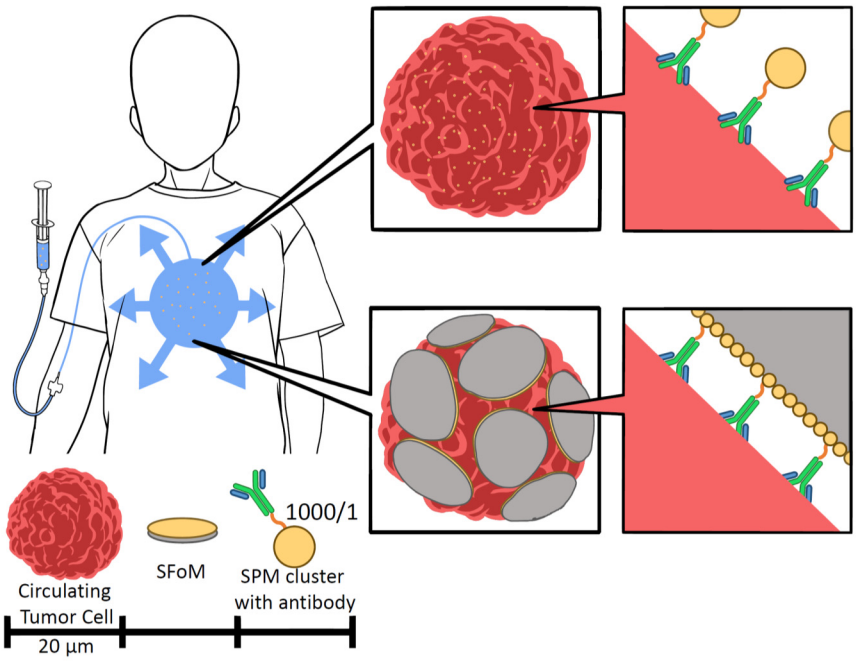

Figure S3. The schematic plot showing a comparison of the total magnetic moments for MRI measurements by estimating the total population of magnetic atoms in a commercial MRI contrast agent and that for the SFoM.

Reference

[1] H. Amiri, M. Mahmoudi and A. Lascialfari, Superparamagnetic colloidal nanocrystal clusters coated with polyethylene glycol fumarate: a possible novel theranostic agent, *Nanoscale*, 2011, **3**, 1022-1030.

[2] U. Jeong, X. Teng, Y. Wang, H. Yang and Y. Xia, Superparamagnetic Colloids: Controlled Synthesis and Niche Applications, *Adv. Mater.* 2007, **19**, 33.

[3] R. H. Kodama, Magnetic nanoparticles, *J. Magn. Magn. Mater*. 1999, **200**, 359.

[4] J. L. Dormann, D. Fiorani and E. Tronc, *Magnetic Relaxation in Fine Particle Systems, in Advances in Chemical Physics*, vol. XCVIII, ed. I. Prigogine and S. A. Rice, J. Wiley and Sons, 1997.

[5] John Watt, Grant C. Bleier, Mariah J. Austin, Sergei A. Ivanov and Dale L. Huber, Non-volatile iron carbonyls as versatile precursors for the synthesis of iron-containing nanoparticles, *Nanoscale*, 2017, 9, 6632-6637.

[6] A. H. Lu, E. L. Salabas and F. Schüth, Magnetic Nanoparticles: Synthesis, Protection, Functionalization, and Application, *Angew. Chem., Int. Ed*., 2007, **46**, 1222–1244.

[7] T. C. Monson, E. L. Venturini, V. Petkov, Y. Ren, J. M. Lavin and D. L. Huber, Large enhancements of magnetic anisotropy in oxide-free iron nanoparticles , *J. Magn. Magn. Mater.*, 2013, **331**, 156–161.

[8] Paolo Allia, Marco Coisson, Paola Tiberto, Franco Vinai, Marcelo Knobel, M. A. Novak, and W. C. Nunes, Granular Cu-Co alloys as interacting superparamagnets, *Phys. Rev. B* 2001, **64**, 144420.

[9] E. F. Ferrari, F. C. S. da Silva, M. Knobel, Influence of the distribution of magnetic moments on the magnetization and magnetoresistance in granular alloys, *Phys. Rev. B* 1997, **56**, 6086-6093.

[10] B. Pacakova, S. Kubickova, G. Salas, A. Mantlikova, M. Marciello, M.P. Morales, D. Niznansky, J. Vejpravova, The internal structure of magnetic nanoparticles determines the magnetic response, *Nanoscale*, 2017, **9**, 5129-5140.

[11] M. El-Hilo, Nano-particle magnetism with a dispersion of particle sizes, *J. Appl. Phys.* 2012, **112**, 103915.

[12] J.T. Jang, H. Nah, J.H. Lee, S.H. Moon, M.G. Kim and J. Cheon, Critical Enhancements of MRI Contrast and Hyperthermic Effects by Dopant-Controlled Magnetic Nanoparticles, *Angew. Chem.*, 2009, **121**, 1260-1264.

[13] E.H. Kim, H.S. Lee, B.K. Kwak and B.K. Kim, Synthesis of ferrofluid with magnetic nanoparticles by sonochemical method for MRI contrast agent, *J. Magn. Magn. Mater*., 2005, **289**, 328-330.

[14] M. Sensi and A. Anichini, Unique Tumor Antigens: Evidence for Immune Control of Genome Integrity and Immunogenic Targets for T Cell-Mediated Patient-Specific Immunotherapy, *Clin. Cancer Res.*, 2006, **17**, 5023-5032.

[15] C. Guo et al., H1N1 influenza virus epitopes classified by monoclonal antibodies, *Ther. Med.,* 2018, **16**, 2001-2007.

[16] I. Roitt and P.J. Delves, *Encyclopedia of Immunology*, 2nd ed. Academic Press (1998).

[17] M. Miyauchi, T.J. Simmons, J. Miao, J.E. Gagner, Z.H. Shriver, U. Aich, J.S. Dordick and R.J. Linhardt, Electrospun Polyvinylpyrrolidone Fibers with High Concentrations of Ferromagnetic and Superparamagnetic Nanoparticles, *ACS Appl. Mater. Interfaces*, 2016, **3**, 1958-1964.

[18] X. Yin, S.E. Russek, G. Zabow, F. Sun, J. Mohapatra, K.E. Keenan, M.A. Boss,

H. Zeng, J.P. Liu, A. Viert, S.H. Liou and J. Moreland, Large T1 contrast enhancement using superparamagnetic nanoparticles in ultra-low field MRI, *Sci Rep.*, 2018, **8**, 11863.

[19] K.E. Kellar, D.K. Fujii, W.H. Gunther, K. Briley-Saebo, A. Bjornerud, M. Spiller, S.H. Koenig, NC100150 Injection, a preparation of optimized iron oxide nanoparticles for positive-contrast MR angiography, *J. Magn. Reson. Imaging*, 2000, **11**, 488-494.

[20] S.C. Yang, C.H. Huang, C.T. Tsou and C.Y. Lin, Manufacturing process of wafer thinning, United States Patent. US 10026603B2 (2018).

[21] B.N.G. Sajay, C.P. Chang, H. Ahmad, W.C. Chung, P.D. Puiu and A.R.A. Rahman, Towards an optimal and unbiased approach for tumor cell isolation, *Biomed. Microdevices*, 2013, **15**, 699-709.